AD-A071 942 STANFORD UNIV CALIF EDWARD L GINZTON LAB F/G 20/12
ACOUSTIC WAVE MEASUREMENTS OF SEMICONDUCTOR PARAMETERS. (U)
JUN 77 G S KINO N00014-75-C-0632
UNCLASSIFIED GL-2709 NL

| OF |
AD
A071942

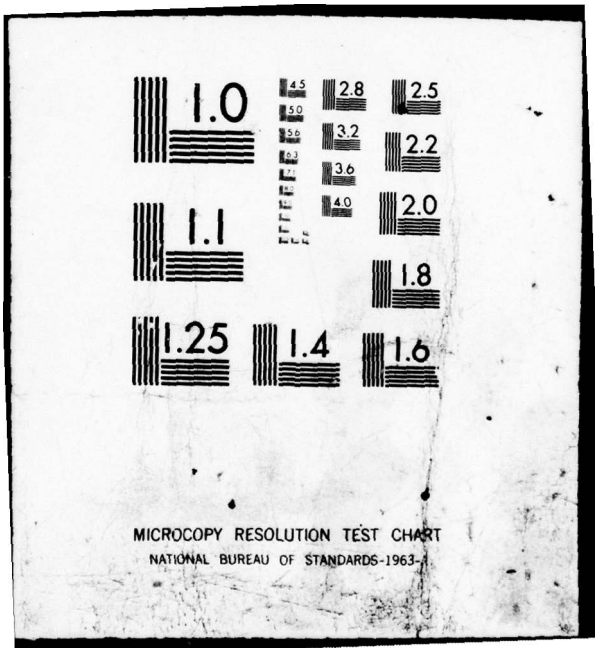
1.0
1.1
1.25
1.4
1.6
1.8
2.0
2.2
2.5
2.8
3.2
3.6
4.0
4.5
5.0
5.6
MICROCOPY RESOLUTION TEST CHART
NATIONAL BUREAU OF STANDARDS-1963-A

ACOUSTIC WAVE MEASUREMENTS OF SEMICONDUCTOR PARAMETERS

by

Gordon S. Kino

INVITED PAPER

INTERNATIONAL SYMPOSIUM ON MICROWAVE
DIAGNOSTICS AND SEMICONDUCTORS

Porvoo, Finland

July 13-15, 1977

G.L. Report No. 2709

June 1977

32p.

Contracts:

NSF Grant No. ENG75-18681

and

ONR Contract N00014-75-C-0632

VNSF-ENG75-18681

409 640

Edward L. Ginzton Laboratory
W. W. Hansen Laboratories of Physics
Stanford University
Stanford, California

ACOUSTIC WAVE MEASUREMENTS OF SEMICONDUCTOR PARAMETERS

by

Gordon S. Kino
Edward L. Ginzton Laboratory
Stanford University
Stanford, Ca. 94305
U.S.A.

ABSTRACT

Various types of acoustic surface wave techniques for measuring the parameters of a semiconductor are discussed in this paper. These include techniques to measure mobility, carrier density, surface state density, and trapping time in surface states.

I. Introduction

During the last five years, a number of researchers throughout the world have been investigating the interaction of acoustic surface waves with a semiconductor. Three typical configurations which are employed for this purpose are those shown in Figs. 1, 2, and 3.[1] The basic purpose is to obtain an interaction between the electric field associated with a Rayleigh wave propagating along the surface of a piezoelectric material and a neighboring semiconductor. Typically, the neighboring semiconductor is spaced from the surface of a slab of $LiNbO_3$, with a spacing of the order of 2000 Å. In some cases, the semiconductor is deposited on the surface of the $LiNbO_3$, as in Fig. 3; in others, like that illustrated in Fig. 4, a piezoelectric material such as ZnO is deposited on the surface of a semiconductor such as silicon. Interaction may take place with either rf electric fields parallel or normal to the surface of the semiconductor. Which is the strongest type of interaction will depend on the resistivity of the material and the thickness of the semiconducting layers.

In most of the work associated with these types of interactions, the

interest has mainly been in measuring acoustic wave attenuation or amplification due to interaction of the acoustic wave with drifting carriers, or alternatively, to measure nonlinear effects between two signals inserted at opposite ends of the device. This latter phenomenon has a large range of applications to signal processing in the so-called acoustic convolvers and surface wave storage correlators. However, in carrying out research on these devices, a great deal of theory was developed in order to obtain a full quantitative understanding of their operation. The use of such theory necessitated a detailed knowledge of the semiconductor properties being employed. So, almost perforce, it was necessary to measure the semiconductor properties; and it was found during the course of the experiments that, in fact, acoustic measurements could give decided advantages over the more conventional techniques in determining such semiconductor parameters as the drift mobility, the carrier density, surface state density, and surface state trapping time. In this paper, we will describe some of these techniques and the results that have been obtained to date.

It should be realized that, although several of the methods used are analogous to the conventional methods of measuring the same parameter, not all have their equivalents.[2,3] Potentially, these techniques could be of great importance, but it must be emphasized that most of them have not been developed as fully as they might be, because the emphasis of the work has not been in that direction. In the long run, such techniques could be developed and could provide methods of measurement with far more flexibility and accuracy than some of those presently employed.

As an example, consider the usual technique for measuring drift mobility. Typically, the measurement is that of Hall mobility, rather than drift mobility.[2] But the two mobilities are not identical and can be, in

particular, quite different in the presence of traps. In fact, the ratio of these two mobilities will vary with frequency when traps are present. Furthermore, the usual Hall mobility measurement is subject to errors due to geometrical effects, and is not always easy to carry out.[2]

An alternative technique is, of course, to measure the carrier density by some independent means, such as the measurement of the capacity of a Schottky diode laid down on the semiconductor, and then determine the drift mobility from the resistivity of the material. Again, this is a somewhat indirect measurement and is not always a convenient one to carry out.[3]

Consider alternative techniques using acoustic surface waves for the direct measurement of drift mobility. When an acoustic surface wave interacts with carriers in a semiconductor, it delivers energy to the carriers. So the acoustic surface wave will be attenuated. Furthermore, there is a second order effect giving rise to a dc current flow along the surface of the semiconductor, the so-called acousto-electric effect. Measurement of either of these effects can give a very good estimate of the drift mobility. Yet a third method can involve applying a dc field to drift the carriers along the surface. It can be shown that, when the drift velocity of the carriers equals the acoustic wave velocity, the attenuation associated with acoustic wave interaction with the carriers becomes zero. Then, as the carrier drift velocity is increased, the attenuation reverses in sign and the acoustic wave is amplified. Thus, by measuring the attenuation as a function of the applied field, one can determine the drift velocity very accurately.

In all these types of measurements, by using an airgap device in which the semiconductor can be removed from the $LiNbO_3$ surface, virgin material, either thermally oxidized of left "bare", can be employed. A disadvantage is that such material samples must be very flat to obtain uniform interac-

tion with the acoustic surface wave. The advantage is that they are not changed by metal electrodes or other materials deposited on them and are available for further use after the measurement has been made. A further advantage of acoustic measurements of all types is that they are conveniently made at relatively high frequencies, typically 100 MHz or more, so that measurements of drift mobility, carrier density, and so on, can be carried out at frequencies much higher than typical surface state trapping rates. In addition, with the configurations shown, it is possible to apply either a dc voltage or a pulsed voltage to an electrode on the back of the $LiNbO_3$, as shown in the configurations of Figs. 2 and 4, and thus affect the carrier density and the surface state density at the surface. In this case, the measurements are taken without using metal electrodes deposited on the surface of the semiconductor itself.

We will now summarize some of the various measurement techniques that have been employed, or might be possible, and give a description of some of the experiments which have been carried out in this field.

II. Measurement of Drift Mobility by the Acoustoelectric Effect

Consider a one dimensional situation when an electric field E is applied to a thin semiconductor with mobility μ, carrier density n, and thickness d. The current per unit width I, which flows along the semiconductor is

$$I = \mu q n E d \tag{1}$$

where q is the electron charge. Now suppose the carrier density is of the form $n = n_0 + n_1 \exp j\omega t$. Then we can write, from the one dimensional form of the equation of continuity:

$$\frac{dI_1}{dx} + j\omega q n_1 d = 0 \tag{2}$$

where we have assumed that the carrier charge is q and may be positive or negative, and where to first order:

$$I_1 = \mu q n_0 E_1 d \tag{3}$$

where μ is the carrier mobility.

For an acoustic wave, I_1 and E_1 vary approximately as $\exp j(\omega t - kz)$, where $k = \omega/v_a$ and v_a is the velocity of the acoustic wave. It follows from Eqs. (2) and (3), therefore, that

$$n_1 = \mu n_0 E_1 / v_a \tag{4}$$

Suppose now we expand Eq. (1) to second order and keep only dc terms. It then follows that there will be a dc current I_0 associated with the rf applied field, which is of the form

$$I_0 = \frac{1}{2} RE(\mu q d n_1 E_1^*) , \tag{5}$$

or, as will be seen from Eq. (4):

$$I_0 = \frac{\mu^2 q d n_0 |E_1|^2}{2 v_a} . \tag{6}$$

Alternatively, if we leave the semiconductor open circuited and measure the potential developed along the length ℓ, we find that this is

$$V_0 = \frac{I_0 \ell}{q d n_0 \mu} = \frac{\mu |E_1|^2 \ell}{2 v_a} \tag{7}$$

Equation (6) can be stated in a more convenient form when it is realized that the power dissipated by the acoustic wave is $P = \ell \mu q d n_0 |E_1|^2/2$. So we can write

$$I_0 = \mu P / \ell v_a . \tag{8}$$

This is a form of the Weinreich relation.[4] It follows that by measuring the power absorbed from the acoustic wave by the semiconductor and the acousto-electric current flowing along it, when it is externally short

circuited, the mobility and sign of the carrier charge can be determined.

This measurement was first carried out with acoustic surface waves by Bers, Cafarella, and Burke,[5] who measured the drift mobility in an accumulation layer in the configuration shown in Fig. 5. They used 30,000 ohm-cm material and varied the surface density of carriers from very low values of the order of a few times $10^{10}/cm^2$ to a few times $10^{11}/cm^2$ by applying a potential to a place on the other side of the $LiNbO_3$. Their measurement of the silicon mobility as a function of surface density is shown in Fig. 6. In their case, they were able to work with a much lower surface carrier density than is normally possible with alternative methods. It can be seen that, with very low surface densities, the mobility of the carriers approached the full mobility of the bulk carriers. When the density is high enough for these measurements to be checked by other techniques, they are in reasonably good agreement with them. The results serve to point out the power of this technique and its applicability in situations where it is difficult to measure mobility by any other technique.

Before proceeding to the discussion of other techniques, one further point should be noted about the acousto-electric technique for measuring mobility; this is that the acousto-electric current associated with power absorption of the acoustic wave depends on the sign of the drift mobility. Thus, it is simple to differentiate between drifting holes and drifting electrons by this technique. So experiments have been carried out to determine not only the mobility but the nature of the carriers contributing to the power absorption of the acoustic wave.[6,9] If two types of carriers are present, in principle, a knowledge of the carrier densities would be required. In practice, at least with the III-V materials, the electron effects tend to be dominant as in Hall effect measurements; so one tends to

observe the electron mobility in an intrinsic material and only observe the hole mobility when the hole density is much larger than that of the electrons.

III. Measurement of Mobility by Measurement of Drift Velocity

This method of measurement is particularly suitable for measurement of the mobility of carriers in thin films, such as silicon on sapphire, or vacuum deposited indium antimonide or cadmium selenide.

We suppose that the drift mobility of free carriers in the material is μ and the Hall mobility μ_H. Normally μ_H and μ differ by a factor near unity.[2] When an electric field is applied in an FET configuration to a thin film semiconductor, the carrier density will change. When, in addition, an electric field E_x is applied in a direction parallel to the surface of the semiconductor, the carriers drift along the semiconductor and the induced current per unit width is

$$I = \mu_{FE} Q E_x , \tag{9}$$

where Q is the total induced charge per unit area. So it follows that

$$Q = qnd = \epsilon E_y \tag{10}$$

where μ_{FE} is called the field effect mobility, and E_y is the electric field normal to the semiconductor. Normally $\mu_{FE} \neq \mu$, because there are trapped carriers present, so some of the induced carriers are stored in traps and are not free to move. The ratio μ_{FE}/μ will vary with the frequency ω of the applied gate field E_y, because the trapping rate varies with frequency.

Another way of writing of the relation betwenn μ_{FE} and μ is in terms of the fraction f of free carriers. We call n_f the number of free carriers per unit volume, and the number in traps n_t per unit volume. Then

we can write

$$n_f + n_t = n \tag{11}$$

and

$$\frac{n_f}{n} = f \tag{12}$$

with

$$I = q\mu n_f E_x d \tag{13}$$

Hence, it follows that

$$\frac{\mu_{FE}}{\mu} = \frac{n_f}{n} = f . \tag{14}$$

When an acoustic measurement of interaction between drifting carriers in a semiconductor and an acoustic surface wave is made, it can be shown that, without traps present, the rf current associated with the acoustic wave is, to first order,

$$I_1 = \mu q n_1 E_0 d + \mu q n_0 E_1 d . \tag{15}$$

where E_0 and E_1 are the dc and rf fields in the x direction, respectively.

Assuming a wave in which the rf field varies as $\exp j(\omega t - kz)$, where $k \approx \omega/v_a$ and v_a is the velocity of the acoustic wave, the equation of continuity [Eq. (2)] yields the result

$$I_1 \approx q n_1 v_a d . \tag{16}$$

So it follows from Eqs. (14) and (15), that

$$I_1 = \frac{\mu q n_0 E_1 d}{(1-v_0/v_a)} , \tag{17}$$

where $v_0 = \mu E_0$.

It will be observed that when $v_0 < v_a$, i.e., the drift velocity of the carriers is less than that of the acoustic velocity, the current associated with the rf field is in phase with the rf field. Hence, power

is absorbed from the acoustic wave. On the other hand, if the drift velocity of the carriers is such that $v_0 > v_a$, the drift current is out of phase with the rf field and power is delivered to the acoustic wave. So the acoustic wave amplitude grows along the length of the device. Thus, by carrying out a careful measurement of the field for which there is neither absorption nor growth, i.e., no power exchange between the acoustic wave and the semiconductor, one can determine the drift velocity v_0 of the carriers very accurately. In practice, this measurement is made with an airgap device by putting the semiconductor in place and removing it. Alternatively, with a material like InSb, the temperature of the material is increased until the carrier density becomes so high that the semiconductor forms a short circuit and absorbs no power from the wave, thus making it possible to calibrate the system.

We now consider what occurs in the presence of traps. We suppose that the traps are deep traps with a density N_t per unit volume, with an energy level $\mathcal{E}_t$ below the Fermi level $\mathcal{E}_F$, which is itself well below conduction band level $\mathcal{E}_C$. In this case, it has been shown by Moore and Smith,[10] that, if N_C is the density of the states in the conduction band, then in thermal equilibrium $f = f_0$, where

$$f_0 = \frac{n_f}{n} = \left[1 + \frac{N_t}{N_C} \exp(\mathcal{E}_C - \mathcal{E}_t)/kT\right]^{-1} . \tag{18}$$

More generally, in the presence of an rf field, the ratio $f = n_f/n$ changes and the relaxation equation for the number of carriers in the traps n_t can be written in the form

$$\frac{\partial n_t}{\partial t} = \frac{n_t}{\tau_t} + \frac{n_f}{\tau_f} \tag{19}$$

where τ_t , τ_f are associated with carrier exchange from the traps to the conduction band, and vice versa. We note that, in equilibrium $\partial n_t/\partial t = 0$, so that

$$\tau_t = \tau_f n_{t0}/n_{f0} = \tau_f(1-f_0)/f_0 \tag{20}$$

It can then be shown by writing $n_t = (1-f)n$, and assuming that the rf carrier density varies as $\exp j\omega t$,

$$f(\omega) = \frac{f_0+j\omega\tau}{1+j\omega\tau} \tag{21}$$

where $\tau = \tau_t\tau_f/(\tau_t+\tau_f)$.

We note that $f(\omega) \to f_0$ as $\omega \to 0$, and $f(\omega) \to 1$ as $\omega \to \infty$, i.e., the number of free carriers is not affected by the presence of traps when the rf frequency is much larger than the relaxation frequency.

The expression for acoustic gain and loss in the presence of traps has been derived by Uchida and by Moore and Smith, who first made measurements of the effects, using bulk waves in CdS.[10,14] It is shown in their papers that v_0 has to be replaced by an effective drift velocity, or drift mobility μ_D in Eq. (16), where

$$\frac{\mu}{\mu_D} = \mathrm{Re}(1/f) = \frac{f_0+\omega^2\tau^2}{f_0^2+\omega^2\tau^2} \tag{22}$$

We note that as $\omega \to 0$, $\mu_D/\mu \to f_0$. As $\omega \to \infty$, $\mu_D/\mu \to 1$. It will be noted that, in fact, the parameter μ_D , which we have called the effective drift mobility in Eq.(22) is idential to the field mobility μ_{FE} , already defined in Eq.(14). The shape of the gain curve as a function of field is also changed by the presence of the traps.[10] This effect has not been utilized in measurement, but presumably could be.

Coldren, using vacuum deposited InSb on $LiNbO_3$,[11] has carried out careful measurements of these effects and correlated them with theory. He

carried out careful Hall measurements on the same film, so he measured the Hall mobility μ_H , rather than the true mobility μ . Typical measurements taken by using the Hall effect to determine μ_H and n_f are shown in Fig. 7 . It will be seen that all these parameters and their ratios vary with temperature. At room temperature, the Fermi level ρ_F is just above ρ_T , so that the defects are not all ionized, but there are more ionized defects than shallow donors, so the trapping is quite significant. As the temperature is lowered, ρ_F moves up and the number of ionized defects becomes very small, so that $n_f \rightarrow n$. Furthermore, if the temperature is increased, the effects are reversed and we find that $n_f \ll n$, and, hence, $\mu_D \ll \mu$.

By using this simple kind of theory, and carrying out the measurements at a single frequency, Coldren was able to obtain a theoretical fit to the measured μ_D/μ_H data as a function of termperature, as shown in Fig. 8. By measuring the internal gain of such an amplifier at different frequencies, he was able to determine how μ_D varied with frequency. To do this, he plotted curves of the type shown in Fig. 9. It will be seen that there is a variation of mobility of approximately 1.3 in the frequency range from 105 MHz to 525 MHz . More careful measurements of this type, then, could lead to a technique for measuring the effective value of τ , the relaxation time.

It should be noted, then, by varying frequency and/or temperature, one can obtain a great deal of information about the nature of the traps. However, it is also worthwhile pointing out that the theory presented here is given in very simplified form. In most materials of this kind, there is a distribution of traps over band gap. So the theory does not give very good information on the trapping time, for there is not always a single trap

level. However, acoustic techniques can even be used, as we shall see later, to find this trap distribution.

Before proceeding to describe some of these techniques, it is worth mentioning that a further possible trap measurement technique could be to measure the noise of an amplifier and correlate the results with theory. It can be shown from Shockley-Read statistics that one source of noise is due to trapping.[11,12] This source of noise can be correlated with the trapping theory. From these results, noise output as a function of frequency and drift voltage can be determined. In InSb samples, this was done by Coldren and he was able to determine, in his frequency range, that $f(\omega) \sim 0.7$ and to predict the variation of the noise figure with this voltage quite accurately.[11,12] Later results with better quality materials, such as silicon on sapphire, given by Ralston, give very good agreement with the noise theory and indicate, on this basis, a very low trap density level.[13] Thus, further development might lead to an interesting technique for measuring trap density by measuring noise levels. This, of course, is a technique that is also applicable in FET amplifiers.

As we have already mentioned, the basic technique for measuring trapping by acoustic methods were originally worked out by Uchida[14], and Moore and Smith,[10] who used volume waves in CdS . Here, because the piezoelectric coupling coefficient is very large relative to surface wave interactions, the measurement is even simpler. When a drift field is applied, the current is proportional to the applied voltage. But, as the drift field is increased beyond the point where the drift velocity equals the acoustic velocity, the current saturates due to the nonlinear effects associated with the acoustic amplification. In this case, then, all that was needed was to measure an I-V characteristic and determine where it saturated to determine the drift

velocity of the carriers. Using the same trapping theory that has been given, Moore and Smith were able to make detailed measurements of trapping effects in CdS .

IV. Measurement of Carrier Density and Surface State Density Using Nonlinear Effects in the Acoustic Convolver

A common method of measuring the carrier density of semiconductors is to deposit an electrode on the semiconductor and measure the capacity of the Schottky diode so formed as a function of the applied voltage. We will describe here an analogous acoustic technique. The field at the surface of a semiconductor, when the depletion layer is formed, is

$$E_y = qN_d \ell/\epsilon \ , \tag{23}$$

where ℓ is the length of the depletion layer, ϵ is the dielectric constant, $C = \epsilon/\ell$ is the capacity per unit area of the diode, N_d is the donor density, and the potential developed across the depletion layer is $\phi = qN_d\ell^2/2\epsilon$. It follows that

$$\phi = \epsilon E_y^2/2qN_d \ . \tag{24}$$

Now suppose that, with a given dc potential ϕ_0 or dc field $E_y = E_0$ applied at the surface of the semiconductor, a small rf perturbation of field is introduced. We note that, if the rf field is of the form $E_{y1} = E_1 \cos \omega t$, then

$$\phi = \frac{\epsilon(E_0+E_1 \cos \omega t)^2}{2qN_D} \tag{25}$$

By averaging over one rf cycle, we see that there is a change in the dc component of the potential at the surface due to the presence of the rf signal of value

$$\Delta\phi_{DC} = \frac{E_1^2\epsilon}{4qN_d} \tag{26}$$

Furthermore, there is a second harmonic component of surface potential generated of value

$$\phi_{2\omega} = \frac{\epsilon E_1^2}{4qN_d} \tag{27}$$

These terms can be measured in a Schottky diode and are used in one technique for measuring carrier density. More generally, this is equivalent to measuring the capacity as a function of voltage and determining the second harmonic components of induced potential.

However, the same technique lends itself very well to acoustic measurements. When an acoustic surface wave is propagated along a piezoelectric substrate near a neighboring semiconductor, as in the configuration of Fig. 1 , a dc potential is generated at the surface of the semiconductor proportional to the square of the rf electric field, or to the power in the acoustic wave. This effect is known as the tranverse acousto-electric effect.[7] By pulsing the rf signal, it is possible to determine this effective induced potential at the surface of the semiconductor. Due to the capacity between the electrode on the other side of the piezoelectric material and the semiconductor, a pulse signal will be picked up on the electrode. Thus, with suitable calibration, the technique provides a fairly direct method of measuring the carrier density.

The measurements of the second harmonic effect, however, is somewhat easier to implement because of the lower output impedances required. Furthermore, more effort has been devoted to it because of the development of the acoustic convolver.[1] In this case, it is convenient to inject two signals at each end of the semiconductor, whose rf fields at the surface of the semiconductor are $E_{a1} \exp j(\omega t - kz)$, $E_{a2} \exp j(\omega t + kz)$, respectively.

A second harmonic potential

$$\phi_{2\omega} = \epsilon E_{a1} E_{a2} / 4qN_d \qquad (28)$$

will therefore be generated. This potential has no variation in the z direction. Therefore, it is possible to pick up the second harmonic voltage generated by this acoustic interaction on the output electrode. The output obtained at the second harmonic is, in fact, the convolution of the two input signals.

The theory of this interaction over the whole range of surface conditions at the semiconductor surface has been developed by Gautier,[15,16] and correlated with experiments for measuring the carrier density. This process has beer examined by several researchers because it is basic to the operation of the so-called acoustic convolver. In general, the relationship between $\phi_{2\omega}$ and the electric fields at the surface of the semiconductor can be written in terms of the dc potential at the surface, i.e., in terms of the dc carrier density at the surface of the semiconductor. The results given here are only valid for well-depleted surface layers. Even in this case, because there is a capacity between the $LiNbO_3$ surface and the semiconductor, it is as if there are two capacities in series; that between the $LiNbO_3$ and the semiconductor, and that of the depletion layer. Therefore, the effective field at the carriers changes with the depletion width, and so a further effect due to the change in the thickness of the depletion layer occurs.

At flatband, the effective depletion layer width is the Debye length λ_d, and it can be shown that there is a decrease in the potential generated by a factor of $1/3$ from that in a depletion layer. In accumulation or inversion, the generated potentials drop considerably because they are inversely proportional to the carrier density [Eq.(28)]; but are predictable.

Some results obtained by Gautier for the convolution efficiency, i.e., the ratio of the output power to the products of the two input power, are shown in Figs. 10 and 11. These results are given as a function of the bias voltage applied to the plate, which varies the carrier density at the surface from accumulation to inversion. Along with these results, the attenuation of the wave as a function of bias is shown; this effect is due to the parallel component of field E_x at the surface.

It will be noted that there is a difference between the results with dc bias and pulse bias, as would be expected. This is due to the fact that there are surface states present. So the technique also gives a method of measuring surface state density.

Gautier has developed the theory in detail and has compared his experimental results for the voltage output as a function of bias, which is proportional to the parameter $\mathcal{M}$, shown in Fig. 11.[15,16] Good agreement is obtained between theory and experiment as far as the second harmonic generation is concerned, except in the inversion region. The reason for this is due to the presence of surface states. By measuring the voltage shift, one can determine the surface state density, just as with the more conventional measurement techniques.[17,18] Gautier did this for both p-type and n-type semiconductors, and obtained the results for surface state density through the bandgap shown in Fig. 12. These results are in reasonable agreement with other measurement techniques. So it will be seen that his technique gives a completely independent method of measuring surface state density. If Gautier's technique were developed further, it could provide more detailed information than other techniques which are available, basically because of its flexibility. As none of the techniques presently used seem to be completely reliable and are open to argument, it remains to be seen which of these methods is most

accurate.

One further point should be noted about this kind of technique. We observe that the acoustic losses predicted by Gautier in this experiment were not in very good agreement over all the range of surface potential with his experimental measurements. In the inversion region, this is because with weak inversion it is difficult to predict exactly the penetration depth of the fields into the inversion layer. So there are some theoretical errors in his results.

However, when the surface is depleted, the number of carriers near the surface is relatively small. So one would normally expect the loss to be lower than at flatband, as is predicted by Gautier's theory.[15,16] In practice, this is not so because of the real part of the admittance due to the presence of surface states.[8,19] Moll has worked out a theory on this basis.[19] We give here a development of this theory to calculate surface state density, which has the same dependence on the parameters as the theory given by Moll.

It has been shown by Nicollian and Goertzberger[17] that, if there is a distribution of surface state density through the band, and there are $N_{SS}/eV\text{-}cm^2$ surface traps, the admittance due to these surface traps is

$$Y_{SS} = \frac{qN_{SS}}{2\tau_m} \ln(1 + \omega^2\tau_m^2) + \frac{jqN_{SS}}{\tau_m} \tan^{-1}\omega\tau_m \qquad (29)$$

where

$$\tau_m = \frac{1}{\sigma v_{th} n_{SO}} \qquad (30)$$

and n_{SO} the density of carriers of either type at the surface, and σ the cross section of the trap at the surface for this type of carrier, with v_{th} the thermal velocity of the carriers. Typically, the trapping times

τ_m are very long compared to the period of the rf signal.

The real part of the admittance for high frequency waves can be written in the form

$$G_{SS} \approx \frac{qN_{SS}\sigma v_{th} n_{SO}}{2} \ell n(\omega^2 \tau_m^2) \tag{31}$$

The power lost per unit area by the acoustic wave due to the presence of this surface state conductance is, therefore

$$P_L = \frac{qN_{SS}\sigma v_{th} n_{SO} \phi_1^2}{2} \ell n(\omega^2 \tau_m^2) \tag{32}$$

where ϕ_1 is the rf potential at the surface of the semiconductor.

Moll, in his analysis, finds an expression for the power lost by writing the normal component of current in terms of the surface recombination velocity v_C. This current is

$$J_1 = qn_{S1} v_C \tag{33}$$

where n_{S1} is the rf carrier density at the surface, and

$$n_{S1} = qn_{SO}\phi_1/kT \tag{34}$$

Thus the power loss per unit area is

$$P_L = q^2 v_C n_{SO} \phi_1^2/2kT \tag{35}$$

Equating Eqs. (32) and (35), we find an effective surface recombination velocity of value

$$v_C = \sigma v_{th} (kTN_{SS}/q) \ell n(\omega^2 \tau_m^2) . \tag{36}$$

On the basis of Eq. (35), Moll has worked out the acoustic loss as a function of the depletion length. It will be seen from Fig. 13 that he obtains a dependence of the loss as a function of the depletion length which varies in essentially the right way; the value of v_C he assumes is measurable when predicted by Eq.(36). This theory predicts, then, a far higher

loss than one would expect if surface state theory were not taken into account. Thus, this technique, if developed, could give rise to yet another method of measuring surface state density. It is obviously very close in concept to the conductance method of measuring surface state density and decay times.

V. Storage Effects

Acoustic wave techniques give rise to methods of measuring decay times in surface states directly,[20,21] as well as measuring storage effects in p-n diodes[22] and Schottky diodes.[23] We will deal here only with the surface state effect as perhaps the most interesting one, although the extrapolation to the same storage effects in p-n diodes and Schottky diodes is of more technical importance.

We have noted already that the convolution effect depends on the applied dc potentials, which, in turn, affects the dc surface potential at the semiconductor. If surface states are present, it follows that the potential at the surface of the semiconductor will change with time after a pulse is applied. Thus, by measuring the convolution output as a function of time after application of a long pulse, and then after removal of the pulse, one can determine charging times and decay times in surface states. The convolution output itself will depend directly on the rf capacity of the depletion layer, and, therefore, on the dc potential developed across the depletion layer.

Experiments of this type were carried out by Quate, Otto, and Moll,[24] who showed that, when an intense rf pulse was inserted into one end of an acoustic surface wave device placed near a semiconductor, the rectification of the rf pulse in the depletion layer caused the depletion layer to be depleted, as shown in Eq. (26). Hence, the attenuation for small signals

changes, because the distance between the carriers and the piezoelectric substrate increases. This attenuation persists for some time because of the presence of surface states, the persistence time depending on the charging rate of the surface states.

An experiment was set up by Hayakawa and Kino[21] to measure this charging time, which is basically the τ_m given in Eq.(30). They used 10 ohm-cm n-type siliscon in the convolver configuration shown in Fig. 2. They injected a short intense rf pulse of the order of 1 watt at one end of the device. This depeleted the surface. The charge time of the traps was changed by varying the depletion level of the surface with a dc bias applied between the silicon and the metal electrode on the other side of the $LiNbO_3$. The device was then operated with smaller signal inputs as a convolver, and the convolution output was measured. The convolution output increased with time, after the application of the large input pulse as the surface states charged up, the charge in the traps reached their equilibrium value and the depletion layer decreased in thickness. By measuring the time for the convolution output to reach a value 1 dB below its equilibrium value, the value of τ_m was measured as a function of the bias voltage.

The results obtained are shown in Fig. 14. It can be seen that, as we have already observed, the insertion loss and convolution output are functions of the bias voltage, as is the storage time. It can be seen that the storage time varied exponentially with the bias voltage, as would be expected. By calculating the potential at the surface, it is possible to predict where the mid-gap potential occured, and to extrapolate the results to the mid-gap potential. From these results, it was possible to estimate the surface state density as being approximately $10^{11}/cm^{-2}$, and the cross section for trapping electrons to be $\sigma = 2 \times 10^{-16} cm^{-2}$; a result in good

agreement with those of Nicollian and Goertzberger. We note that the storage times observed were in the range from 50 μsec to 2 msec.[21]

VI. Conclusions

We have described a number of acoustic techniques for measuring mobility, density, trapping time, surface state density, and surface state density distribution. Most of these techniques are not well developed because the effort has been towards development of devices rather than to the development of measurement techniques. It is apparent that most of the techniques have analogs in more conventional methods, but the acoustic methods have the advantage that they are operated at very high frequencies and can be used to measure material surfaces free of all other electrodes. The material can then be used for other purposes. Obviously a more careful use of these techniques could prove very fruitful for measurements of semiconductors.

ACKNOWLEDGEMENT

The author would like to thank J. Moll and L. Coldren for use of some of their unpublished results.

The author's work reported in this paper was supported in part by the National Science Foundation under Grant No. ENG75-18681, and in part by the Office of Naval Research under Contract N00014-75-C-0632.

REFERENCES:

1. G. S. Kino, "Acoustoelectric Interactions in Acoustic Surface Wave Devices," Proc. IEEE, Special Issue on Surface Acoustic Wave Devices and Applications, 64, No. 5, pp. 724-748, May 1976
2. R. A. Smith, "Semiconductors," Cambridge University Press, 1961.
3. S. M. Sze, "Physics of Semiconductor Devices," John Wiley and Sons, Inc. 1969.
4. G. Weinreich, "Acoustodynamic Effects in Semiconductors," Phys. Rev., 104, 321, 1956.
5. A. Bers, J. H. Cafarella, and B. E. Burke, "Surface Mobility Measurements Using Surface Acoustic Waves," Appl. Phys. Lett., 22, pp. 399-401, April 1973.
6. F. Das, M. E. Malamedi, and R. T. Webster, "Determination of Semiconductor Surface Properties Using Surface Acoustic Waves," Appl. Phys. Lett. 27, pp. 120-122, Augusut 1975.
7. Y. V. Gulyaev, A. Y. Karabanov, A. M. Kmita, A. V. Medved, and S. S. Tursunov, "Theory of Electronic Absorption and Amplifications of Surface Acoustic Waves in Piezoelectric Crystals," Sov. Phys.-Solid State, 12, pp. 2085-2090, 1971.
8. T. Shiosaki, T. Kuroda, and A. Kawabata, "Application of Surface Waves to the Study of Semiconductor Surface States Using the Separated-Medium Acoustoelectric Effect," Appl. Phys. Lett., 26, pp. 360-362, 1975.
9. S. Takeda, K. Hoh, H. Hayakawa, and N. Mikoshiba, Proc. 4th Conf. on Solid State Devices, Tokyo, 1972. J. Japan Soc. Appl. Phys. 42, Suppl. (1973), p. 21.

10. A. R. Moore and R. N. Smith, "Effect of Traps on Acoustoelectric Current Saturation in CdS," Phys. Rev., 138, A1250-A1258, May 17, 1965.

11. L. A. Coldren, "Monolithic Acoustic Surface Wave Amplifiers," Ph.D. dissertation, Stanford University, Stanford, Ca., 1972.

12. G. S. Kino and L. A. Coldren, "Noise Figure Calculation for the Rayleigh Wave Amplifier," Appl. Phys. Lett., 22, pp. 50-52, 1973.

13. R. W. Ralston, "Stable CW Operation of Gap-Coupled Silicon-on-Sapphire to $LiNbO_3$ Acoustoelectric Amplifiers," presented at IEEE Ultrasonics Symposium, Los Angeles, Ca., 1975, paper V5.

14. I. Uchida, T. Ishiguro, Y. Sasaki, and T. Suzuki, "Effect of Trapping of Free Carriers in CdS Ultrasonic Amplifier," J. Phys. Soc. Japan, 19, pp. 674-680, May 1964.

15. H. R. Gautier, "Acoustic Wave Semiconductor Convolver Applied to Electrical and Optical Signal Processing," Ginzton Lab., Stanford, Ca., GL Rep. 2448, June 1975.

16. H. Gautier and G. S. Kino, "A Detailed Theory of the Acoustic Wave Semiconductor Convolver," IEEE Trans. on Sonics and Ultrasonics, Su-24, pp. 23-33, January 1977.

17. E. H. Nicollian and A. Goetzberger, "The $Si-SiO_2$ Interface-Electrical Properties as Determined by the Metal-Insulator-Silicon Conductance Technique," Bell Syst. Tech. J., XLVI, pp. 1055-1133, 1967.

18. B. E. Deal, E. L. McKenna, and P. L. Castro, "Characteristics of Fast Surface States Associated with SiO_3-Si and Si_3N_4-SiO_2-Si Structures," J. Electrochem. Soc. 116, pp. 997-1005, 1969.

19. N. J. Moll, "Acoustic Detection of Thermal Radiation," Ph.D. Dissertation, Stanford University, Stanford, Ca. 1977.

20. A. Bers and J. H. Cafarella, "Surface State Memory in Surface Acousto-electric Correlator," Appl. Phys. Lett., 25, pp. 133-135, 1974.

21. H. Hayakawa and G. S. Kino, "Storage of Acoustic Signals in Surface States in Silicon," Appl. Phys. Lett., 25, pp. 178-180, 1974.

22. C. Maerfeld and P. Defranould, and P. Tournois, "Acoustic Storage and Processing Devices Using p-n Diodes," Appl. Phys. Lett., 27, pp. 577-578 1975.

23. K. A. Ingebrigtsen, "The Schottky Diode Acoustoelectric Memory Correlator - A Novel Programmable Signal Processor," Proc. IEEE, Special Issue on Surface Acoustic Wave Devices and Applications, 64, No. 5, pp. 764-769, May 1976.

24. N. J. Moll, O. W. Otto, and C. F. Quate, "Scanning Optical Patterns with Acoustic Surface Waves," J. Phys., 33, Colloque C-6, Suppl. pp. 231-234, 1972.

FIGURE CAPTIONS

1. A schematic of an "airgap" amplifier with silicon-on-sapphire spaced from $LiNbO_3$ by thin SiO rails.
2. A schematic of an "airgap" silicon convolver spaced by SiO rails.
3. A schematic of an acoustic amplifier using a film of InSb vacuum evaporated on to $LiNbO_3$.
4. A schematic of a ZnO on Si convolver.
5. Experimental configurations used for mobility measurements.
6. Silicon mobility as a function of electron sheet density and surface potential measured by Bers, et al.[5]
7. Plots of n , n_f , σ , μ_D , μ_H versus reciprocal temperature.
8. Theoretical fit to the experimental μ_D/μ_H data as a function of termperature.
9. Electronic gain versus drift voltage with frequency as a parameter.
10. Experimental measurement of convolution efficiency (F_T) and propagation loss (L_S) vs bias voltage (V_G), for
    (a) an n-type silicon on YZ $LiNbO_3$ convolver. The full line curve corresponds to the dc bias measurements; the dashed line curve to the pulsed bias measurement.
    (b) a p-type silicon on YZ $LiNbO_3$ convolver (dc bias only)[15,16]
11. $\mathcal{M}$-value and propagation loss vs bias voltage (p-type silicon). The dots are the experimental points. The full line curve corresponds to the complete theory; the dashed line curve to the theory in the absence of surface states near the conduction band edge.[15,16]
12. Surface state density of $Si-SiO_2$ structure as obtained from
    (a) by Gautier.[15,16]
    (b) by Nicollian and Goetzberger.[17]
    (c) by Castro and Deal.[18]

13. Theoretical and experimental data for the attenuation coefficient vs. depletion width. The silicon is n-type, spaced 2500 Angstroms from a lithium niobate delay line. The frequency is 100 MHz; the silicon is taken to have a carrier concentration of 2×10^{14} cm^{-3} and a capture velocity of 1.8×10^{4} cm/sec. The experimental data is that of Gautier.[15,16] The plot is by Moll.[19]

14. Storage time, convolution output, and insertion loss as a function of bias voltage. The convolution output and the insertion loss are normalized by taking values without bias as references.[21]

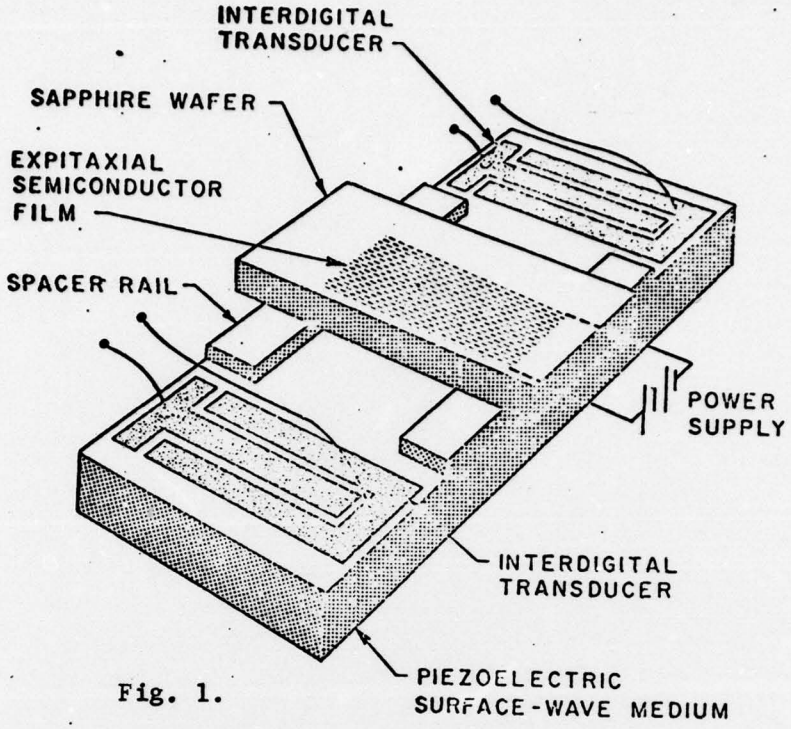

Fig. 1.

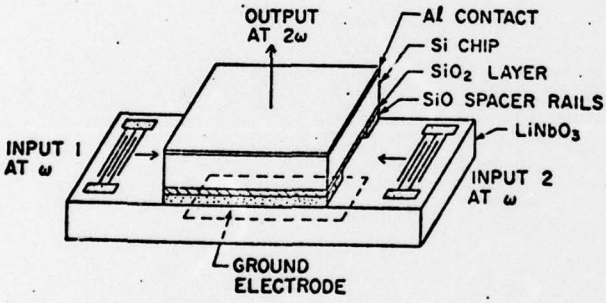

Fig. 2

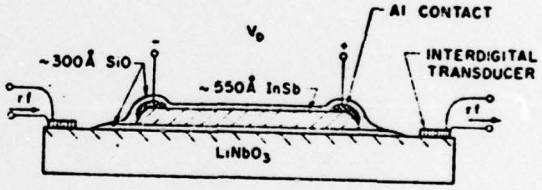

Fig. 3

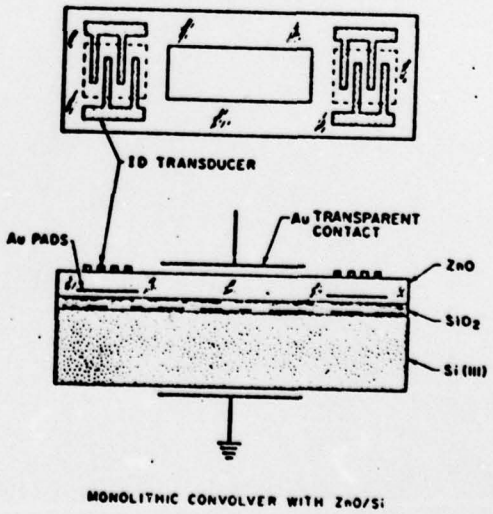

Fig. 4

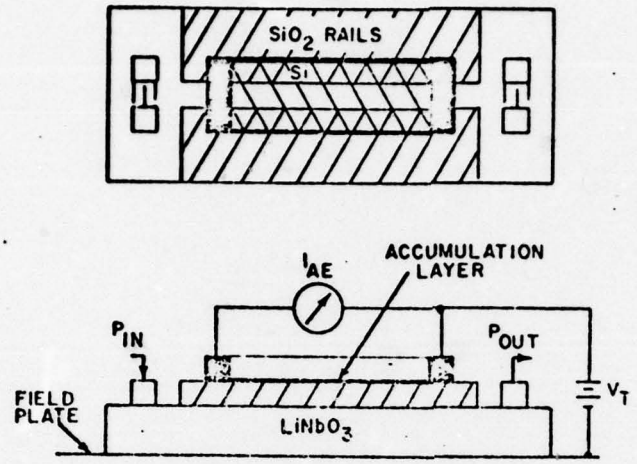
SiO_2 RAILS
Si
I_{AE}
ACCUMULATION LAYER
P_{IN}
P_{OUT}
V_T
FIELD PLATE
$LiNbO_3$

Fig. 5

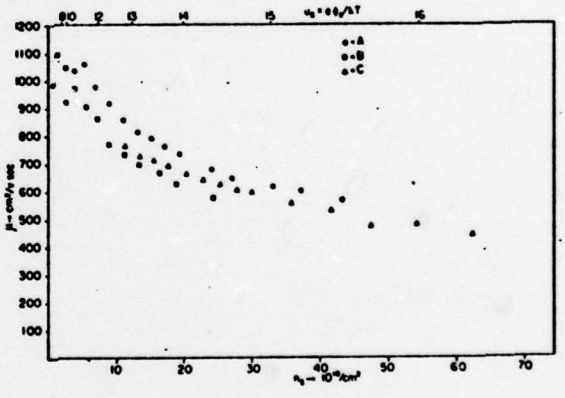
A
B
C

Fig. 6

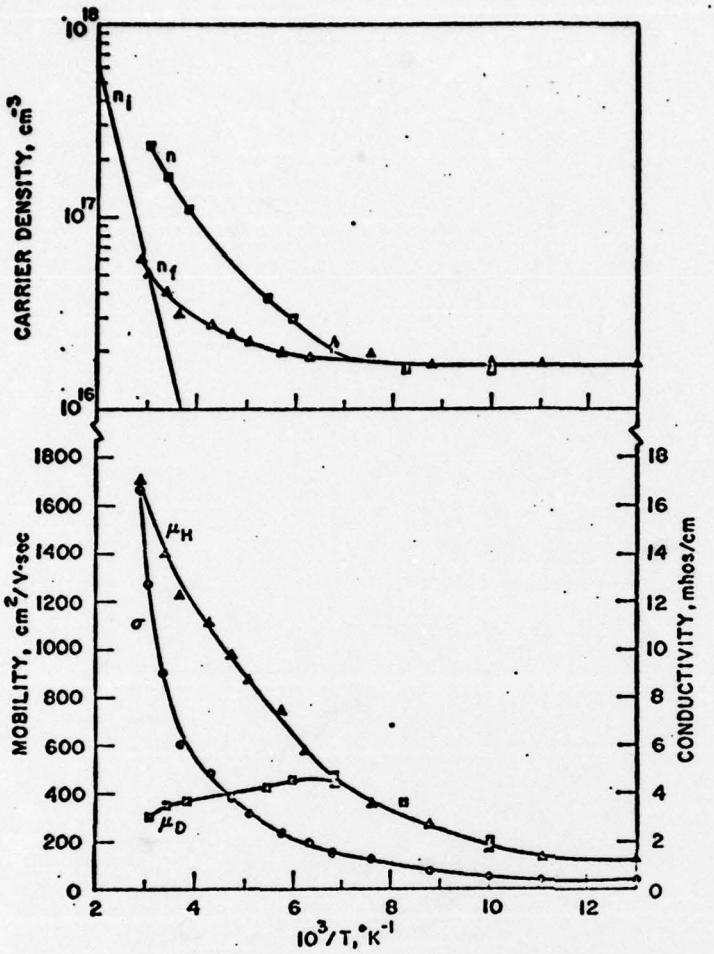

Plots of n , n_f , σ , μ_D , μ_H versus reciprocal temperature.

Fig. 7

μ_D/μ_H vs T

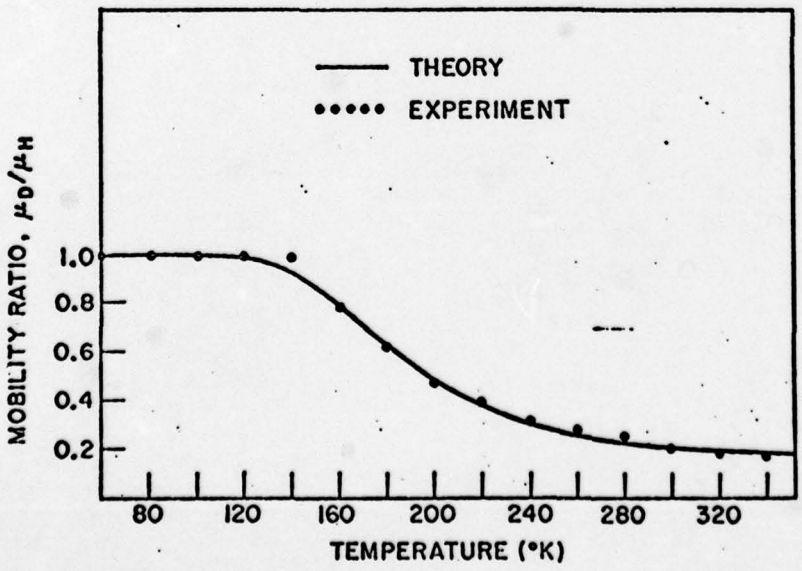

Fig. 8

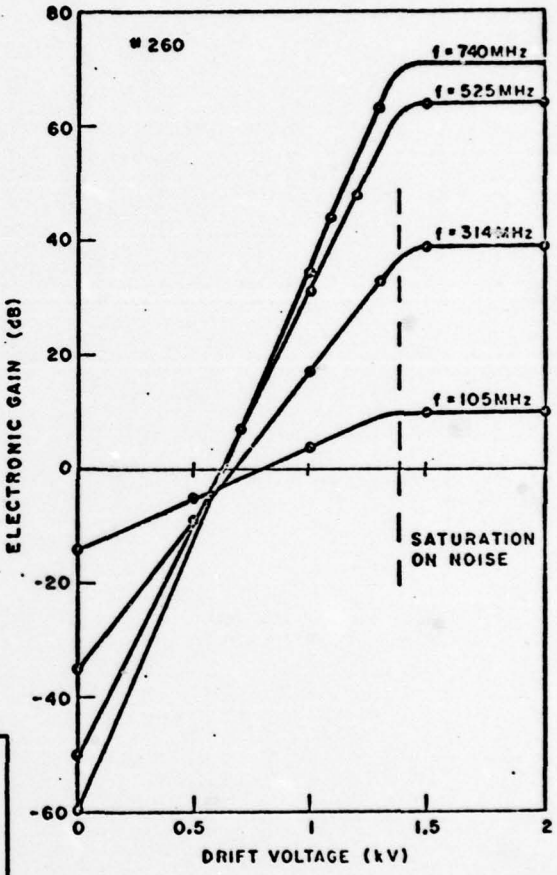

Fig. 9

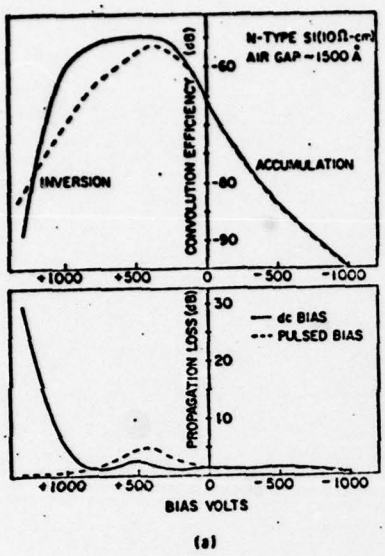

(a)

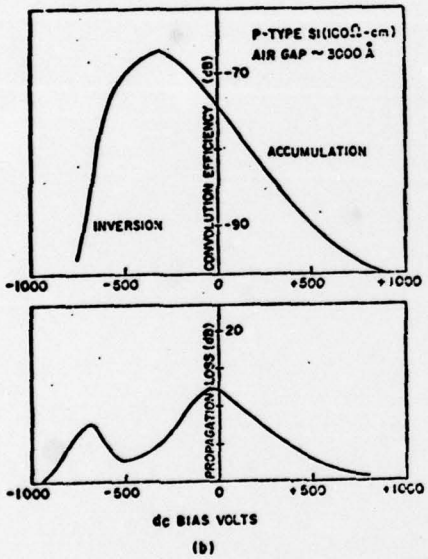

(b)

Fig. 10

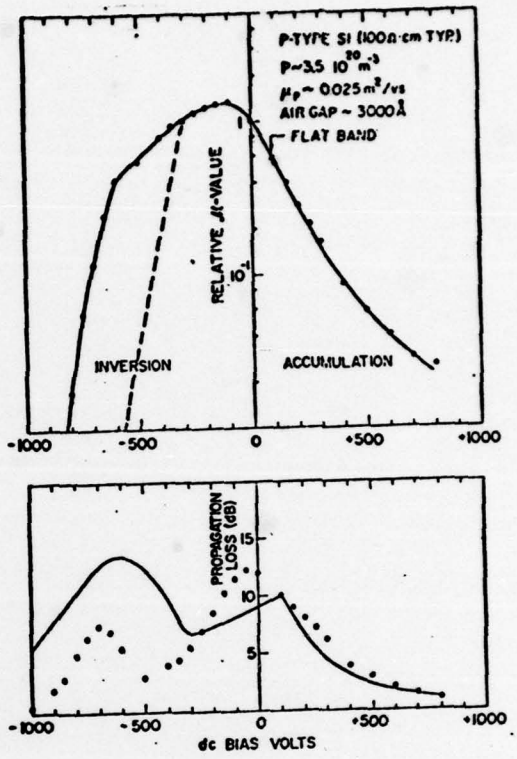

Fig. 11

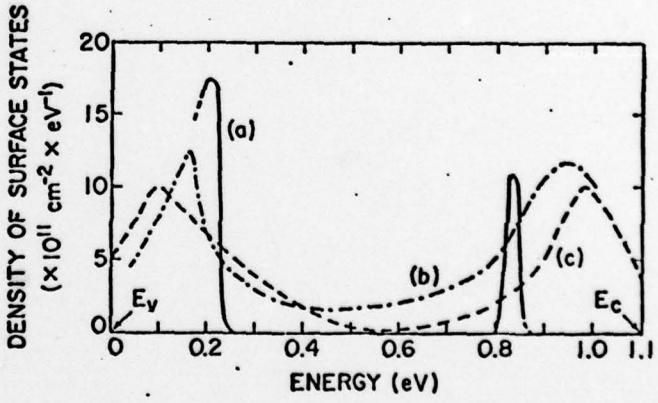

Fig. 12

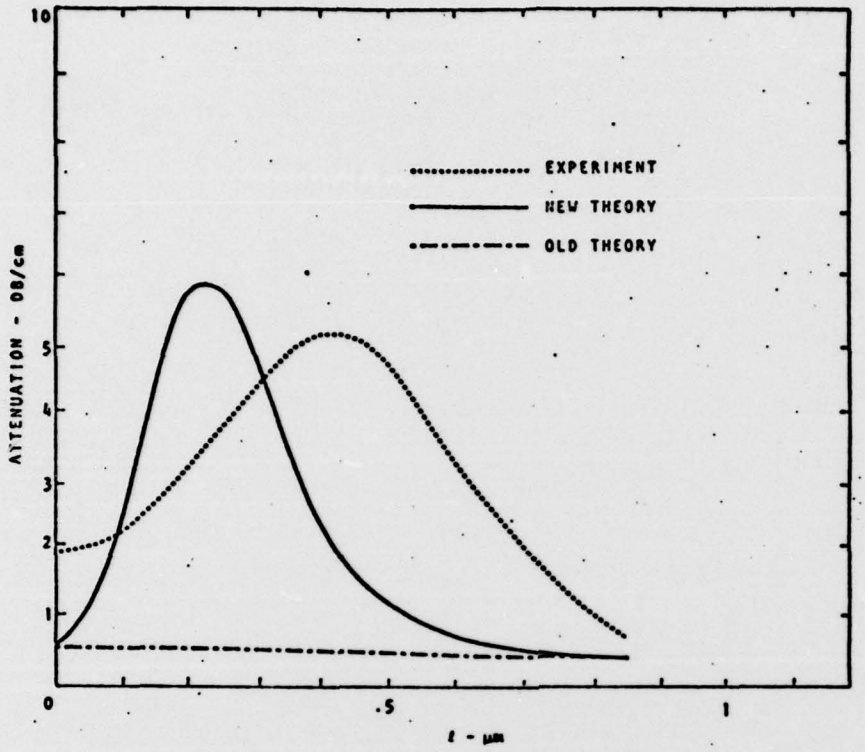
EXPERIMENT
NEW THEORY
OLD THEORY
ATTENUATION - DB/cm
10
5
4
3
2
1
0
.5
1
ℓ - μm

Fig. 13

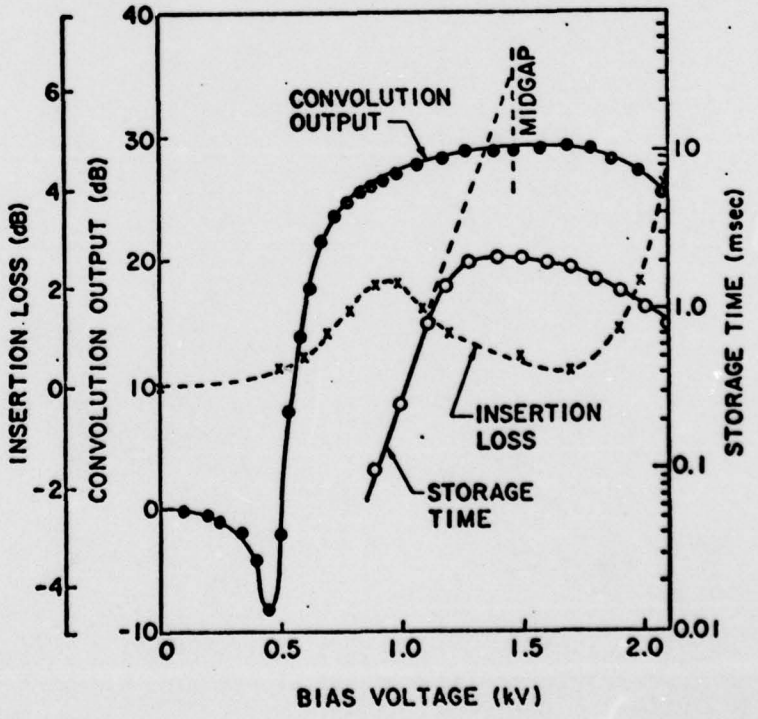
CONVOLUTION OUTPUT
MIDGAP
INSERTION LOSS
STORAGE TIME
INSERTION LOSS (dB)
CONVOLUTION OUTPUT (dB)
STORAGE TIME (msec)
BIAS VOLTAGE (kV)
40
30
20
10
0
-10
6
4
2
0
-2
-4
10
1.0
0.1
0.01
0
0.5
1.0
1.5
2.0

Fig. 14